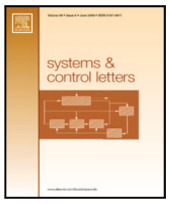
Systems & Control Letters 196 (2025) 106015



Contents lists available at ScienceDirect

Systems & Control Letters

journal homepage: www.elsevier.com/locate/sysconle



Command governor schemes for dynamical systems subject to rate-bounded disturbances

Francesco Tedesco *, Gianfranco Gagliardi, Alessandro Casavola

DIMES, University of Calabria, Via Ponte Pietro Bucci, Rende, 87036, Cosenza, Italy

ARTICLE INFO

Keywords:
Command governor
Rate-bounded disturbance
Set-theoretic approach

ABSTRACT

This paper extends the well-known Command Governor (CG) scheme to the case of rate-bounded persistent disturbances acting as exogenous signals on the plant. The methodology is founded on a multimodal supervisory unit that, during online operations, effectively orchestrates the switching among various CG configurations. These configurations are pre-designed offline based on the magnitude of disturbance occurrences to satisfy the prescribed constraints. To achieve this, a customized notion of *transition dwell-time* is incorporated within the proposed supervisory framework to determine the necessary duration to facilitate safe transitions among operational modes without compromising constraint satisfaction. Simulation results on two different linear systems indicate that the multimodal CG architecture is markedly less conservative when compared to the traditional single CG scheme.

1. Introduction

Reference tracking in dynamical systems subject to input and/or state constraints is a fundamental problem in automatic control theory. The most known approach to deal with such a problem is represented by the Model Predictive Control (MPC) [1] which usually requires to re-design the existing control architecture (if already present on the plant). An alternative way relies on introducing into the existing control loop an add-on device with constraints handling capability. Such a methodology is denoted in literature as the Reference Governor (RG) or Command Governor (CG) approach. A CG unit is a nonlinear static device that, in tracking control problems, modifies a desired reference sequence when its application would produce pointwise-in-time set-membership constraints violation on relevant variables of the closed-loop system. On the contrary, the modified reference sequence is the best approximation of the original one with respect to some selection index and ensures by design that all operative constraints [2,3] are satisfied along the system evolutions driven by the modified reference sequence.

Similarly to MPC techniques, the solution of the CG design problem makes use of future system predictions and the key advantage is the limited computational burden of the online phase with respect to the MPC computations. For a comprehensive survey on the subject, please refer to [4,5].

Moving from these considerations, in this paper, we will assume that disturbances acting on the plant are characterized by a rate-bounded magnitude. Such an assumption has been considered in [6–8], with the aim of reducing the conservativeness of existing control laws at the price of a slightly more complicated design. This paper shows that, even for CG strategies, less conservative schemes can be designed with enlarged admissible solution sets. The main idea used here is to decompose the bounding region where the disturbance is confined, into several nested inner sub-sets. Then, a multimode supervisory scheme is adopted to orchestrate the switching among dedicated CG units for each sub-set via a suitable switching logic. The latter is in charge of safely orchestrating the transitions among such CG units on the basis of a disturbance subset membership condition, that can be estimated online from measurable system variables. Therefore, the main area of investigation here is identifying guaranteed circumstances under which *safe* CG switchings can occur. In the proposed framework, this is achieved by jointly resorting to viability arguments and the dwell-time notion [9], here used to determine the minimum amount of time that a transition between two adjacent CG configurations has to last.

Multimode CG or RG based architectures have been presented in recent years for dealing with several issues. In [10], a RG scheme has been designed to remotely manage a system that switches between two feedback control laws. Such an idea has been generalized in [11], where a multimode RG scheme capable of computing an admissible virtual reference within several faulty configurations was proposed. Furthermore, a hybrid CG scheme has been presented in [12] to deal with time-varying constraints.

* Corresponding author.
E-mail addresses: ftedesco@dimes.unical.it, francesco.tedesco@unical.it (F. Tedesco).

https://doi.org/10.1016/j.sysconle.2024.106015
Received 26 October 2023; Received in revised form 9 December 2024; Accepted 26 December 2024
Available online 11 January 2025
0167-6911/© 2025 The Authors. Published by Elsevier B.V. This is an open access article under the CC BY license (http://creativecommons.org/licenses/by/4.0/).

Differently from the above mentioned works, this paper shows how a multimode CG architecture can be exploited to deal with rate-bounded disturbance signals. As one of its main merits, the proposed strategy rigorously allows one to online select the least conservative CG configuration able to safely comply with the prescribed constraints according to the current disturbance level.

The paper is organized as follows. In Section 2, the standard CG design problem is stated and its solution presented. In Section 3, the novel proposed CG scheme dealing with rate bounded disturbances is introduced and its relevant properties proved. In Section 4, an illustrative final example is presented.

A preliminary version of this work was presented in [13], where the strategy was applied to constrained load-frequency control problems in multi-area power grids. The current paper significantly extends this prior work by formally introducing the problem, providing detailed proofs for all theoretical results, and presenting a new illustrative example that demonstrates how the proposed approach enlarges the set of admissible initial states compared to the traditional method.

Preliminaries and notations

$\mathbb{R}$, $\mathbb{R}_+$ and $\mathbb{Z}_+$ denote respectively the real, non-negative real and non-negative integer numbers. The Euclidean norm of a vector $x \in \mathbb{R}^n$ is denoted by $\|x\| = \sqrt{x_1^2 + \cdots + x_n^2}$ whereas $\|x\|_\Psi^2, \Psi = \Psi^T > 0$, denotes the quadratic form $x^T \Psi x$. A generic ball in an Euclidean n-space $\mathbb{R}^n$ is defined as $\mathcal{B}_\delta := \{x \in \mathbb{R}^n : \|x\| \le \delta\}$. The boundary of a compact set $\mathcal{A}$ is defined as $\partial(\mathcal{A})$. 0_n is the zero vector of $\mathbb{R}^n$.

Definition 1.1 (*Minkowski Sum*)**.** Given the sets $\mathcal{A}, \mathcal{E} \subset \mathbb{R}^n$, $\mathcal{A} \oplus \mathcal{E} := \{a + e : a \in \mathcal{A}, e \in \mathcal{E}\}$ is *Minkowski set sum*.

Definition 1.2 (*Pontryagin–Minkowski Difference*)**.** Given the sets $\mathcal{A}, \mathcal{E} \subset \mathbb{R}^n$, $\mathcal{A} \sim \mathcal{E} := \{a : a + e \in \mathcal{A}, \forall e \in \mathcal{E}\}$ is *the Pontryagin–Minkowski set difference*.

2. Problem formulation

Consider the following linear, time-invariant representation of the plant regulated by the primal controller as in Eq. (1)

$$\begin{cases} x(t+1) &= \Phi x(t) + G g(t) + d(t) \\ y(t) &= H_y x(t) \\ c(t) &= H_c x(t) + L g(t) \end{cases} \tag{1}$$

with $x(t) \in \mathbb{R}^n$ the state vector (which includes the controller states); $g(t) \in \mathbb{R}^m$ the manipulable reference which, if no constraints were present, it would essentially coincide with the reference $r(t) \in \mathbb{R}^m$; $y(t) \in \mathbb{R}^m$ the output, viz. a performance related signal; $c(t) \in \mathbb{R}^{n_c}$ the constrained vector

$$c(t) \in C, \ \forall t \in Z_+ \tag{2}$$

with $C \subset \mathbb{R}^{n_c}$ a prescribed convex and compact set. Finally

$$d(t) \in D \subset \mathbb{R}^d, \ \forall t \in \mathbb{Z}_+ \tag{3}$$

with D a known convex and compact set with $0_d \in D$, is a not measurable exogenous input sequence contained in D, whose magnitude is rate-bounded, i.e.

$$|\|d(t+1)\| - \|d(t)\|| \le \bar{\Delta}_d, \forall t \in \mathbb{Z}_+. \tag{4}$$

Please notice that simple rate-bounded sequences are included in the class of signals defined by means of (4). In fact,

$$\begin{array}{ccc} \|d(t+1) - d(t)\| & \le & \bar{\Delta}_d, \forall t \in \mathbb{Z}_+ \\ & \Downarrow & \\ |\|d(t+1)\| - \|d(t)\|| \le & \|d(t+1) - d(t)\| \le & \bar{\Delta}_d, \forall t \in \mathbb{Z}_+ \end{array}$$

It is assumed that

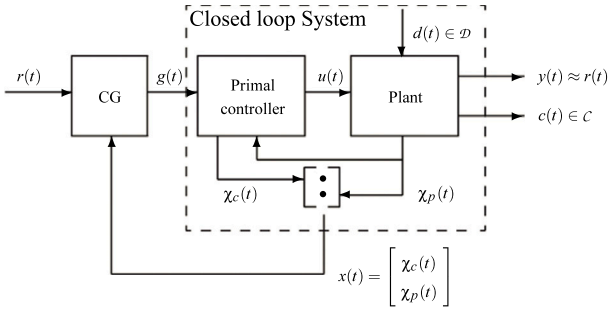


Fig. 1. The CG control scheme for system (1).

$$(A1)\begin{cases} (1) & \Phi \text{ is Schur matrix;} \\ (2) & \text{System (1) is offset-free w.r.t. } g(t), \text{ i.e.} \\ & H_y(I_n - \Phi)^{-1} G = I_m \end{cases}$$

The CG design problem consists of generating, at each time instant t, the command $g(t)$ according to a static feedback law that depends on the current state $x(t)$ and reference $r(t)$

$$g(t) := \underline{g}(x(t), r(t)) \tag{5}$$

This law should be able to guarantee, under suitable conditions, the satisfaction of the constraints (2) for all possible disturbance realizations $d(\cdot) \in D$ and a yet satisfactory tracking performance ($y(t) \approx r(t)$, the best given the constraints).

2.1. Classic Command Governor design

The traditional solution of [2] for the above stated problem is depicted in Fig. 1 and it does not address the possible rate-boundedness on the signal $d(t)$. For this reason, the resulting scheme is based on a worst-case approach where $d(t)$ can take all possible values within the set D at each time instant.

By linearity, one is allowed to separate the effects of the initial conditions and inputs from those of disturbances, $x(t) = \bar{x}(t) + \tilde{x}(t)$, where $\bar{x}(t) := \Phi^t x(0) + \sum_{i=0}^{t-1} \Phi^{t-i-1} G g(i)$ is the disturbance - free component and $\tilde{x}(t) := \sum_{i=0}^{t-1} \Phi^{t-i-1} d(i)$ depends only on the disturbances. Then, we adopt the following notations

$$\begin{array}{lcl} \bar{x}_g & := & (I_n - \Phi)^{-1} G g \\ \bar{y}_g & := & H_y (I_n - \Phi)^{-1} G g \\ \bar{c}_g & := & H_c (I_n - \Phi)^{-1} G g + L g \end{array} \tag{6}$$

for the disturbance-free equilibrium solutions of (1) to a constant command $g(t) \equiv g$.

Hence, the main idea is to choose at each time instant a constant virtual vector $g(\cdot) \equiv g$, such that the corresponding virtual evolution fulfills the constraints over a semi-definite horizon. Moreover, it is required that the discrepancy between the command $g(t)$, generated by the CG unit, and the nominal reference $r(t)$ is the minimal possible.

To this end, compute the following Minkowski difference recursions on the constrained set C

$$C_0 := C, C_k := C \sim \Xi_k, \quad \ldots, C_\infty := C \sim \Xi_\infty \tag{7}$$

where $\Xi_1 := H_c D$, $\Xi_k := \Xi_{k-1} \oplus H_c \Phi^{k-1} D$, $k > 1$ and Ξ_∞ represents the Hausdorff limit [14] of the sequence Ξ_k. Because of Schur nature of Φ, it can be proved (see [15,16]) that Ξ_∞ is convex and compact and that, provided all C_k are non-empty, they are also convex and compact, satisfy the nesting condition $C_k \subset C_{k-1}$ and make C_∞ a nonempty, convex, compact and finitely determinable set. By exploiting the previously presented achievements, a CG device can be designed for the plant (1) by only considering disturbance-free predictions of the system and adopting a "worst-case" approach. As shown in [2], this CG unit is able to compute at each time instant its command $g(t)$ by using

the following selection rule

$$J(g, r(t)) := \|g - r(t)\|_{\Psi}^2 \tag{8}$$

as a cost in the following convex quadratic optimization problem

$$g(t) := \arg \min_{g \in \mathcal{V}(x(t))} J(g, r(t)) \tag{9}$$

where

$$\mathcal{V}(x) = \left\{ g \in \mathcal{W}_\delta \,:\, \bar{c}(k, x, g) \in \mathcal{C}_k,\ \forall k \in \mathbb{Z}_+ \right\} \tag{10}$$

with

$$\bar{c}(k, x, g) = H_c \bar{x}(k, x, g) + Lg \tag{11}$$

$$\bar{x}(k, x, g) = \Phi^k x + \sum_{i=0}^{k-1} \Phi^{k-i-1} G g \tag{12}$$

$$\mathcal{W}_\delta := \left\{ g \in \mathbb{R}^m \,:\, \bar{c}_w \in C^\delta \right\}, \mathcal{C}_\delta := \mathcal{C}_\infty \sim \mathcal{B}_\delta \tag{13}$$

In (13), $\mathcal{B}_\delta$ denotes a ball of radius δ centered at the origin. It represents the set of all constant virtual sequences in $\mathcal{W}_\delta$, whose evolutions starting from x satisfy the constraints also during transients. It can also be shown that such a set is finitely determined, viz. there exists a positive integer k_0 such that (10) is identically characterizable by restricting $k \in \{0, \dots, k_0\}$, with k_0 computable off-line as described in [17]. In this respect, the choice of δ has effects on the finite determinateness of $\mathcal{V}(x(t))$ influencing the value of the integer k_0, the smaller δ, the larger k_0.

The main properties concerning feasibility, stability and computability of the above described CG can be found in [2].

Theorem 1. *Consider system (1) along with the CG selection rule (9). Let assumptions (A1) be fulfilled and $\mathcal{V}(x(0))$ be non-empty. Then:*

1. *The minimizer in (9) uniquely exists at each $t \in \mathbb{Z}_+$ and can be obtained by solving a convex constrained optimization problem, viz. $\mathcal{V}(x(0))$ non-empty implies $\mathcal{V}(x(t))$ non-empty along the trajectories generated by the CG command (9).*
2. *The set $\mathcal{V}(x(t))$, $\forall x(t) \in \mathbb{R}^n$, is finitely determined, viz. there exists an integer k_0 such that if $\bar{c}(k, x(t), g) \in \mathcal{C}_k$, $k \in \{0, 1, \dots, k_0\}$, then $\bar{c}(k, x(t), g) \in \mathcal{C}_k$ $\forall k \in \mathbb{Z}_+$. Such a constraint horizon k_0 can be determined off-line.*
3. *The constraints (2) are fulfilled for all $d(\cdot) \in \mathcal{D}$.*
4. *The overall system is BIBO stable; in particular, whenever $r(t) \equiv r$, $\lim_{t\to\infty} g(t)$ converges in a finite time either to r or to its best steady-state admissible approximation*

$$\hat{r} := \arg \min_{g \in \mathcal{W}_\delta} J(g, r) \tag{14}$$

Consequently, by the offset-free condition (A1.2), $\lim_{t\to\infty} \bar{y}(t) = \hat{r}$, where $\bar{y}$ is the disturbance-free component of y.

Remark 1. In this paper, we do not look at conditions that ensure $\mathcal{C}_\infty$ being not empty. Situations where $\mathcal{C}_\infty$ is found to be empty are hard to be anticipated. This might indicate the use of overly conservative constraints or an unrealistic disturbance model. In such a case, the CG approach is simply inapplicable since the problem is ill-posed (typically it arises when the set $\mathcal{D}$ is too large and/or the set $\mathcal{C}$ is too tight). In practice, this means that the set $\mathcal{V}(x)$ is empty for any x. In this respect, the conditions under which $\mathcal{C}_\infty$ is guaranteed to be non-empty are outlined in the Refs. [15,16], offering a framework for robust constraint designs.

3. Supervisory multimode CG architecture

Here, the additional condition (4) on the rate bounded disturbance is taken into account by properly modifying the standard CG approach of Section 2.1. It will be shown that the new CG scheme, hereafter denoted as CG for Rate Bounded Disturbance (RBD-CG), has improved performance.

To this end, the set $\mathcal{D}$ is assumed to be decomposable into l nested subsets $\{\mathcal{D}_i\}_{i=0}^{l-1}$ such that

$$\mathcal{D}_0 := \mathcal{D} \tag{15}$$

$$\mathcal{D}_{i+1} \oplus \mathcal{B}_{\bar{\Delta}_d} \subset \mathcal{D}_i \tag{16}$$

The latter sets are associated with the notion of *Minimum Disturbance Transition Time* (MDTT),

$$\tau_d^i := \inf_{d \in \partial(\mathcal{D}_{i+1})} \{\tau : \{d\} \oplus \tau \mathcal{B}_{\bar{\Delta}_d} \not\subseteq \mathcal{D}_i\} \tag{17}$$

that is the minimum time required for the sequence $d(t) \in \partial(\mathcal{D}_{i+1})$ to get outside the set $\mathcal{D}_i$. In other words, the sequence $d(t)$ spends at least $\tau_d^i - 1$ time instants in $\mathcal{D}_i$ before getting out of it. The idea is to design a dedicated CG unit for each sub-set $\mathcal{D}_i$, $i \in \mathcal{I} := \{0, \dots, l-1\}$ and a global Switching Logic unit, capable to safely orchestrate the transitions among the CG units.

The Multimode CG-based supervisory architecture is sketched in Fig. 2. It basically consists of a **Bank** of l CG units, say it $\{CG_0, CG_1 ..., CG_{l-1}\}$, each one off-line designed by considering the ith disturbance configuration $\mathcal{D}_i$. A specific **Switching Logic** unit is in charge of activating the proper CG_i in order to guarantee the best tracking performance under constraints fulfillment.

More in details, each CG_i is designed on the basis of the procedure presented in Section 2.1 with recursions (7) computed on the particular set $\mathcal{D}_i$ as follows

$$\begin{aligned} \mathcal{C}^i{}_0 &:= \mathcal{C} \\ \mathcal{C}^i{}_k &:= \mathcal{C}^i{}_{k-1} \sim H_c \Phi^{k-1} \mathcal{D}_i \\ &\vdots \\ \mathcal{C}^i{}_\infty &:= \bigcap_{k=0}^{\infty} \mathcal{C}^i{}_k \end{aligned} \tag{18}$$

Accordingly, one finds

$$\mathcal{V}_i(x) = \left\{ g \in \mathcal{W}^i{}_\delta \,:\, \bar{c}(k, x, g) \in \mathcal{C}^i{}_k,\ \forall k \in \mathbb{Z}_+ \right\} \tag{19}$$

where

$$\mathcal{C}^i{}_\delta := \mathcal{C}^i{}_\infty \sim \mathcal{B}_\delta \tag{20}$$

$$\mathcal{W}^i{}_\delta := \left\{ g \in \mathbb{R}^{m+p} \,:\, \bar{c}_w \in \mathcal{C}^i{}_\delta \right\} \tag{21}$$

It is also worth pointing out that, for each CG_i, the set $\mathcal{V}_i(x)$ can be interpreted as the "*slice*" of the Output Admissible Set [3] for the system (1)

$$\mathcal{Z}_i := \left\{ \begin{bmatrix} x \\ g \end{bmatrix} \in \mathbb{R}^n \times \mathcal{W}^i{}_\delta \,:\, \bar{c}(k, x, g) \in \mathcal{C}^i_k,\ \forall k \in \mathbb{Z}_+ \right\} \tag{22}$$

along the direction provided by x.

Moreover, of interest for the forthcoming analysis, let

$$\mathcal{X}_i := \left\{ x \in \mathbb{R}^n \,|\, \exists\, g \in \mathcal{W}^i{}_\delta,\ s.t. \begin{bmatrix} x \\ g \end{bmatrix} \in \mathcal{Z}_i \right\} \tag{23}$$

be the "*slice*" of $\mathcal{Z}_i$ projected onto $\mathbb{R}^n$. It represents the set of all initial states x that can be steered to feasible equilibrium points without constraints violation.

Then, each CG_i unit for the ith disturbance configuration can be simply determined as follows.

$$g(t) = \arg \min_{g \in \mathcal{V}_i(x(t))} \|g - r(t)\|_{\Psi}^2 \tag{24}$$

The **Switching Logic** unit is instructed to trigger a safe transition between two adjacent CG devices according to the set-membership of the current value of $d(t)$ to a set of the family $\{\mathcal{D}_i\}_{i=0}^{l-1}$. It outputs a signal $\sigma : \mathbb{Z}^+ \to \mathcal{I} := \{0, \dots, l-1\}$ that belongs to the class of piecewise constant sequence and is used to orchestrate the switchings between the dedicated CG_i devices. Roughly speaking, at each time instant, this logic seeks for the smallest set $\mathcal{D}_{i^\star}$ among the set family $\{\mathcal{D}_i\}_{i=0}^{l-1}$, such that $d(t) \in \mathcal{D}_{i^\star}$. Then, the $CG_{\sigma(t)}$ becomes active at time t with $\sigma(t) \le i^\star$ in order to guarantee constraints fulfillment.

In view of this, the first aspect to clarify is related to the determination of the disturbance signal set-membership index. Although in

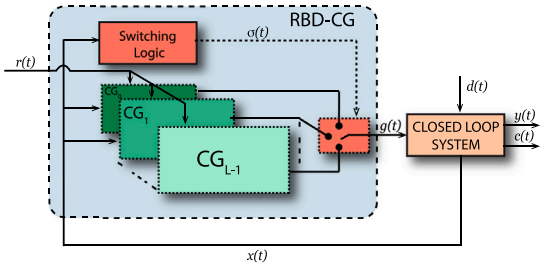


Fig. 2. Supervisory multimode CG architecture for rate-bounded disturbance.

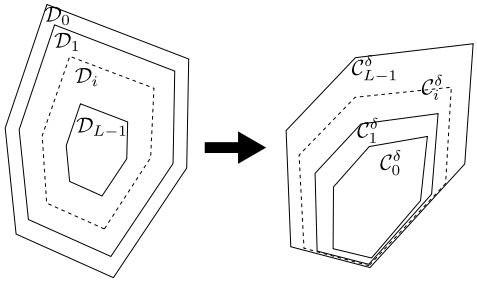


Fig. 3. Graphic representation of Lemma 1.

principle this would require that the disturbance $d(t)$ were known at each time t, our algorithm is able to work fine by exploiting the value $d(t-1)$ at time t. In fact, the latter can be easily derived in the following way

$$d(t-1) = (x(t) - \Phi x(t-1) + Gg(t-1)) \tag{25}$$

without assuming that the disturbance sequence is measurable online.

3.1. Command governor switchability conditions

This subsection investigates the conditions that ensure an admissible switching between any two CG configurations. A first result in this respect is represented by the following Lemma 1 whose graphic idea is depicted in Figure Fig. 3

Lemma 1. *Let $\{\mathcal{D}_i\}_{i=0}^{l-1}$ be a family of nested sets with*

$$\mathcal{D}_{i+1} \subset \mathcal{D}_i \tag{26}$$

and consider the set sequence $\mathcal{C}^i{}_k$, $\forall k$, defined in (18) for a given $\mathcal{D}_i$. Then,

$$\mathcal{C}^{i+1}_k \supset \mathcal{C}^i_k, \forall k \in \mathbb{Z}_+ \setminus \{0\} \tag{27}$$

is found.

Proof. The proof is based on the observation that, thanks to Pontryagin–Minkowski set difference properties,

$$H_c\Phi^k\mathcal{D}_{i+1} \subset H_c\Phi^k\mathcal{D}_i, \forall k \in \mathbb{Z}_+$$

results because of (26). The latter directly implies that

$$\mathcal{C}^{i+1}_k \sim H_c\mathcal{D}_{i+1} \supset \mathcal{C}^{i+1}_k \sim H_c\mathcal{D}_i, \forall k \in \mathbb{Z}_+ \tag{28}$$

that, thanks to recursions (18), is equivalent to (27) □

A direct consequence of Lemma 1 is that the sets $\mathcal{Z}_i$ determined in (22) for each $\mathcal{D}_i$ satisfying (26), are such that

$$\mathcal{Z}_{i+1} \supset \mathcal{Z}_i.$$

Then, for a family $\{\mathcal{X}_i\}_{i=0}^{l-1}$ of sets determined according to (23), the following condition simply follows.

$$\mathcal{X}_{i+1} \supset \mathcal{X}_i, \forall i \in \mathcal{I} \tag{29}$$

In view of these achievements, it is worth pointing out that, during the online operations, if at a certain time instant $\hat{t}$, the following condition holds true

$$d(\hat{t}) \in \mathcal{D}_{i-1}, \tag{30}$$

any kind of switch $CG_{i-2} \to CG_{i-1}$ can be enabled immediately. On the contrary, kind of switches $CG_i \to CG_{i-1}$ started at time t' can be allowed at time $\hat{t}$ only if the following conditions hold true

$$x(\hat{t}) \in \mathcal{X}_{i-1} \tag{31}$$

and

$$d(t) \in \mathcal{D}_i,\ t' \le t < \bar{t},\ \bar{t} \ge \hat{t} \tag{32}$$

In fact, in the latter case, it is required to steer the state trajectory $x(\cdot)$ into $\mathcal{X}_{i-1}$ before the switching event can take place and before the sequence $d(\cdot)$ jumps outside $\mathcal{D}_i$ (within $\mathcal{D}_{i-1}$). Within this context, the introduction of a guard time is necessary. Then, the notion of dwell-time firstly presented in [9] is here presented and properly tailored for the proposed framework.

In particular, in order to guarantee a safe transition between CG_i and CG_{i-1}, $i = 1, \dots, l-1$, it is required to determine the time interval that is necessary to wait for steering any starting state $x(t) \in \mathcal{X}_i$ into $\mathcal{X}_{i-1}$, so that condition (31) is satisfied. To this end, we will make use of the following definition:

Definition 3.1. Let $t_0, t_1, \dots, t_k$ with $0 = t_0 < t_1 < \cdots < t_k$ denote switching instants. The positive constant $\tau_{i,i-1}$ is said the *transition dwell-time* relatively to the commutation from CG_i to CG_{i-1} if

$$t_{k+1} - t_k \ge \tau_{i,i-1}.$$

for all k such that $\sigma(t) = i$ for $t \in [t_k, t_{k+1})$ and $\sigma(t_{k+1}) = i-1$

Remark 2. Note that, because of Theorem 1, $\tau_{i,j} = 0$ when $j > i$. □

The transition dwell-time concept is now specialized to comply with the RBD-CG structure. To this end, let $\mathcal{X}_i$ and $\mathcal{X}_{i-1}$ be the operating compact regions pertaining to CG_i and CG_{i-1}. Then, system (1) is safe under the switching $CG_i \to CG_{i-1}$ if there exists, for each possible initial condition $x(t') \in \mathcal{X}_i$, a quantity τ_i such that for any switching signal with transition dwell times $\tau_{i,i-1} \ge \tau_i$ one has that

$$x(t'+t) \in \mathcal{X}_{i-1},\ t \ge \tau_i \tag{33}$$

Furthermore, for our purposes, we need to identify an upper bound among all possible τ_i values that meet the previously mentioned criteria. Such a quantity, here denoted as *maximal transition dwell-time* (MTDT), can be formally defined as follows:

$$\tau_i^\star := \sup_{x \in \mathcal{X}_i} \inf_{g \in \mathcal{V}_i(x)} \left\{\tau : \bar{x}(k, x, g) \in \mathcal{X}_{i-1},\ \forall k \ge \tau\right\} \tag{34}$$

Please notice that the latter quantity needs to be compatible with the MDTT of (17) in order to satisfy both conditions (30)–(31) at the switching time instant $\hat{t}$. To this end, let us consider the worst case scenario where $\|d(\cdot)\|$ has an increasing trend and

$$|\|d(t+1)\| - \|d(t)\|| = \bar{\Delta}_d, \forall t \in \mathbb{Z}_+. \tag{35}$$

so that $d(t)$ spends exactly $\tau_d^i - 1$ time instants within each set $\mathcal{D}_i$ before proceeding out of it (inside $\mathcal{D}_{i-1}$). In this case, a switch $CG_i \to CG_{i-1}$ needs to be performed before $d(\cdot)$ jumps outside $\mathcal{D}_i$. The following Lemma 2 gives some necessary and sufficient conditions to ensure that these transitions are always safe

Lemma 2. *Any switch from CG_i to CG_{i-1}, $i \in \mathcal{I}$, started at time t' such that $x(t') \in \mathcal{X}_i$, $d(t'-1) \in \mathcal{D}_i$ and enabled at time $\hat{t} \le t' + \tau_i^\star$ is safe, that is both (31)–(32) are satisfied, iff the following conditions hold true*

$$\tau_i^\star < \tau_d^i - 1 \tag{36}$$

and

$$d(t'-2) \in \mathcal{D}_j, j \ge i+1 \tag{37}$$

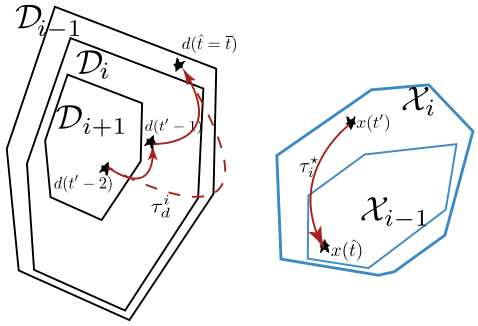


Fig. 4. Graphic idea of Lemma 2.

Proof. (*Sufficiency*) The proof arises by looking at both definitions (17) and (34). In fact, from (34) it is evident that a feasible command g exists at time t' that is able to steer $x(t)$ into $\mathcal{X}_{i-1}$ in at most $\tau_i^\star$ time instants. Therefore, condition (31) is satisfied. Moreover, due to (17), (35) and (37), the signal $d(\cdot)$ can get out of $\mathcal{D}_i$ only at time $\bar{t} = t' + \tau_d^i - 2$. Thanks to (36), one has $\bar{t} = t' + \tau_d^i - 2 \geq t' + \tau_i^\star \geq \hat{t}$. As a consequence, (32) is also fulfilled.

(*Necessity*) Let us consider that $x(t)$ is steered into $\mathcal{X}_{i-1}$ in $\tau_i^\star$ steps. Then, the switching time instant is $\hat{t} = t' + \tau_i^\star$. Let us assume that (32) is also fulfilled. This implies, in the worst case, that $\bar{t} = t' + \tau_d^i - 2 = \hat{t}$. Then $t' + \tau_d^i - 2 = t' + \tau_i^\star$, hence $\tau_d^i = \tau_i^\star + 2$ and, in turn, (36) directly follows. By contradiction, if (37) were not satisfied, because of (35), $\bar{t} < \hat{t}$ would hold true and in turn (32) would be violated. □

Remark 3. The design conditions stated in Lemma 2 are derived in the case that the set-membership of $d(\cdot)$ is detected after one time instant via (25). In the cases where $d(t)$ is measurable at time t, slightly less conservative conditions can be used.

A graphic idea of Lemma 2 can be found in Fig. 4, where the worst case scenario is depicted. In fact, it can be seen that, even in the case where $d(t)$ escapes from $\mathcal{D}_i$ in at most τ_d^i steps starting from $d(t'-2) \in \mathcal{D}_{i+1}$, $x(t)$ is steered in a shorter/equal time interval to $\mathcal{X}_{i-1}$.

The latter Lemma 2 suggests an important expedient to be adopted in the Switching Logic. In fact, given the minimal set-membership index of $d(t-1)$ into $\{\mathcal{D}_i\}_{i=0}^{l-1}$ at time t, the following procedure

$$\begin{aligned} i^\star(t) \quad &:= \quad \arg\max_{i \in \mathcal{I}} i \\ s.t. \quad &\quad d(t-1) \in \mathcal{D}_i \end{aligned} \tag{38}$$

provides a possible, although conservative, way to satisfy condition (37) at each time instant, that consists to maintain the signal $\sigma(t)$ equals to $\max\{0, i^\star(t)-1\}$.

3.2. CG for rate bounded disturbance

Before presenting the online phase of the proposed multimode supervisory strategy, it is assumed that l CG units, each one complying with the corresponding disturbance set $\mathcal{D}_i$, have been designed for system (1) according to the procedure given in the previous Section 3.1 with parameters $\tau_i^\star$ and τ_d^i complying with (36).

Then, the online operations will follow Algorithm 1 hereinafter presented. It consists of two main logic modes: DEFAULT and SWITCH. The variable $s(t) \in \{\texttt{DEFAULT}, \texttt{SWITCH}\}$ is used to store the current active mode. In particular, the DEFAULT mode is active until

$$x(t) \in \mathcal{X}_{i^\star(t)} \tag{39}$$

In this scenario, the reference $g(t)$ is determined according to

$$g(t) = \arg\min_{g \in \mathcal{V}_{\sigma(t)}(x(t))} \|g - r(t)\|_\Psi^2 \tag{40}$$

with $\sigma(t) = \max\{0, i^\star(t)-1\}$. Whenever condition (39) is violated, a *transition* reference g_{sw} is computed as

$$\begin{aligned} g_{sw} \quad &= \quad \arg\min \|g - r(t)\|_\Psi^2 \\ s.t. \quad &\quad g \in \mathcal{V}_{\sigma(t)}(x(t)) \\ &\quad \bar{x}(\tau_d^{i^\star(t)} - 1, x(t), g) \in \mathcal{X}_{\sigma(t)-1} \end{aligned} \tag{41}$$

in order to safely steer the state into $\mathcal{X}_{\sigma(t)-1} \subseteq \mathcal{X}_{i^\star(t)}$. To this end, the SWITCH mode is activated to apply $g(t) = g_{sw}$ while condition (39) is violated.

These simple steps are presented in the following pseudo-code implementation

Algorithm 1: Rate Bounded Disturbance Command Governor (***RBD-CG***) algorithm

```
INPUT: x(t), r(t)
OUTPUT: g(t)
1: if t == 0 then
2:     set σ(t−1) = 0, i*(t) = 0
3: else
4:     determine d(t−1) via (25)
5:     find i*(t) via (38)
6: end if
7: goto s(t)
8: DEFAULT:
9: if x(t) ∈ X_{i*(t)} then                          ▷ (39) is true
10:    σ(t) ← max{0, i*(t) − 1}
11:    solve (40)
12:    goto 26
13: else
14:    σ(t) ← σ(t − 1)
15:    solve (41)
16:    s(t) =SWITCH
17:    goto 7
18: end if
19: SWITCH:
20: if x(t) ∉ X_{i*(t)} then                         ▷ (39) is false
21:    g(t) ← g_sw
22: else
23:    s(t) =DEFAULT
24:    goto 7
25: end if
26: apply g(t);
27: t ← t + 1.
```

3.3. Main properties

The main properties of the **RDB-CG** strategy are summarized in the next Theorem 2.

Theorem 2. *Let the constrained system (1)–(4) be given, assumptions (A1) fulfilled, $x(0) \in \mathcal{X}_{\sigma(0)}$ and $d(0) \in \mathcal{D}_{\sigma(0)}$. Then:*

1. (feasibility) The system (1)–(4) under the action of Algorithm 1 never violates the constraints (2), i.e. $c(t) \in \mathcal{C}, \forall t \in \mathbb{Z}_+$.

2. (stability) for any disturbance sequence $\Pi = d(k)_{k=0}^\infty$ complying with assumption (4), the state $x(t)$ remains confined into the set $\mathcal{X}_{l-1}$, that it is compact if the pair (A, E_c) is observable, where $A := \begin{bmatrix} \Phi & G \\ 0_{m\times n}, & I_{n\times m} \end{bmatrix}$ and $E_c := [H_c, L]$.

3. (convergence) For any disturbance sequence $\Pi = \{d(k)\}_{k=0}^\infty$ complying with assumption (4) and such that $d(k) \in \mathcal{D}_{\bar{l}}$, $\forall t \geq \bar{t}$, whenever $r(t) \equiv r$, the command $g(t)$ converges either to r or to its best steady-state admissible approximation

$$\hat{r} := \arg\min_{g \in \mathcal{W}_\delta^{\bar{l}-1}} J(g, r) \tag{42}$$

Consequently, by the offset-free condition (A1.2), $\lim_{t\to\infty} \bar{y}(t) = \hat{r}$, where $\bar{y}$ is the disturbance-free component of y.

Proof. 1. Under switching-free scenarios, the CG action provided by ***Step*** 11 of Algorithm 1 for the single ith CG is able to ensure viability and constraints satisfaction. On the other hand, a switch $CG_i \to CG_{i+1}$ is always safe thanks to (29) and it is implicitly carried out through ***Steps*** 9 to 11. A critical situation occurs whenever $CG_i \to CG_{i-1}$ switching is required in virtue of ***Step*** 12 at a certain time $t = t'$. This is safely accomplished by ***Step*** 14 that guarantees a safe transition to $\mathcal{X}_{i^\star(t')}$ in at most $\tau_i^\star$ steps within the SWITCH mode. In particular, the existence of solutions for problem (41) is guaranteed by the existence of $\tau_i^\star$ in (34) complying with (36). During this time interval, the constraints fulfillment is ensured by Lemma 2 whose condition (37) is always satisfied with $j = i^\star(t-1)$, $i = \sigma(t)$ thanks to ***Steps*** 10 and 13.
2. From the previous item it directly follows that $(x(t), g(t))$ is confined into $\mathcal{Z}_{l-1}$ and, in turn, $x(t) \in \mathcal{X}_{l-1}, \forall t > 0$. To prove that the sets $\mathcal{X}_i$ are compact it is enough to prove that a generic $\mathcal{Z}_i$ is compact. Because (A, E_c) is an observable pair, the matrix $\Gamma^T\Gamma$ is non-singular, where $\Gamma := [E_c^T, (E_cA)^T, \dots, (E_cA^{n+m-1})^T]^T$. It follows that the linear map between (x, g) and c admits the left inverse operator

$$[x^T, g^T]^T = (\Gamma^T\Gamma)^{-1}\Gamma^T[c^T(0, x, g), \dots, c^T(n+m-1, x, g)]^T$$

3. Because the considered disturbance sequence, after a finite $\bar{t}$, produces samples within a certain set $\mathcal{D}_{\bar{t}}$ the ***Step*** 5 in Algorithm 1 will find $i^\star(t) \equiv \bar{i}$ for all $t \geq \bar{t}$. Within this scenario, thanks to the constraints structure of (41), the condition on ***Step*** 9 becomes true in a finite time $\tilde{t}$. Then, after the time instant $t = \bar{t} + \tilde{t}$, Algorithm 1 will perform ***Steps*** 9−11 within the DEFAULT mode. Therefore, the scheme becomes equivalent to the standard CG scheme of [2] with sets $\mathcal{W}_\delta^{\bar{i}-1}$ and $\mathcal{V}_{\bar{i}-1}(\cdot)$ that enjoys the properties of Theorem 1. □

3.4. Computational aspects

It is evident that the computation of $\tau_i^\star$ by means of (34) is an hard task because the underlying optimization problem is non convex and, as a consequence, computationally demanding to be performed after the determination of set families $\{\mathcal{D}_i\}_{i=0}^{l-1}$ and related $\{\mathcal{Z}_i\}_{i=0}^{l-1}$. To overcome such a technical difficulty, a possible way is to define an iterative procedure to compute at the same time the $\mathcal{D}_i$ decomposition sequence along with the corresponding CG sets by explicitly imposing that the related MDTT and MTDT comply with condition (36). A pseudo-code for implementing such a procedure is hereinafter presented:

Algorithm 2: Procedure for computing $\mathcal{Z}_i$ and $\mathcal{D}_i$

INPUT: $\mathcal{Z}$, $\mathcal{X}$, $\mathcal{D}$, l_{max}, δ, k_0
OUTPUT: l, $\{\bar{\mathcal{Z}}_i\}_0^{l-1}$, $\{\mathcal{D}_i\}_{i=0}^{l-1}$, τ_i, τ_d^i

Let $\mathcal{D}_0 = \mathcal{D}$, $\bar{\mathcal{Z}}_0 := \mathcal{Z}$, $\mathcal{X}_0 := \mathcal{X}$, $i = 1$,
while $\mathcal{B}_{\bar{\Delta}_d} \subset \mathcal{D}_{i-1}$, and $i \leq l_{max}$ **do**
  not found $\leftarrow$ *true*,
  $\tau_i \leftarrow 1$, $\mathcal{D}_i \leftarrow \mathcal{D}_{i-1} \sim \mathcal{B}_{\bar{\Delta}_d}$,
  while *not found* == *true* and $\mathcal{B}_{\bar{\Delta}_d} \subset \mathcal{D}_i$ **do**
    $\tilde{\mathcal{Z}}_i \leftarrow \{[x^T, g^T]^T \in \mathbb{R}^{n+m} | \bar{x}(k, x, g) \in \mathcal{X}_{i-1}, \forall k \geq \tau_i\}$
    compute (18) **with** $\mathcal{D}_i$
    compute $\mathcal{Z}_i$ and $\mathcal{X}_i$
    if $\mathcal{Z}_i \cap \tilde{\mathcal{Z}}_i \neq \emptyset$ **then**
      not found $\leftarrow$ *false*, $\bar{\mathcal{Z}}_i \leftarrow \mathcal{Z}_i \cap \tilde{\mathcal{Z}}_i$
    else
      $\tau_i{+}{+}$, $\mathcal{D}_i \leftarrow \mathcal{D}_i \sim \mathcal{B}_{\bar{\Delta}_d}$
    end if
  end while
  $\tau_d^i \leftarrow \tau_i + 2$, $i{+}{+}$
end while
$l \leftarrow i - 1$

Obviously, the sets in Eqs. (41) and (40) need to be derived from $\bar{\mathcal{Z}}_i$ instead of $\mathcal{Z}_i$. The following Proposition states a useful property of the sets $\bar{\mathcal{Z}}_i$.

Proposition 1. *Let $\{\bar{\mathcal{Z}}_i\}_{i=0}^{l-1}$ be a family of sets determined according to Algorithm 2. Then,*

$$\bar{\mathcal{Z}}_i \supset \bar{\mathcal{Z}}_{i-1}, \forall i \in \mathcal{I} \tag{43}$$

Proof. From ***step*** 10 of Algorithm 2, $\bar{\mathcal{Z}}_i := \mathcal{Z}_i \cap \tilde{\mathcal{Z}}_i$ for $i \geq 1$. Then, the statement of the Proposition for $i > 1$ simply follows from Lemma 1 and condition (29). On the contrary, for $i = 1$ it is required to prove that $\mathcal{Z}_1 \cap \tilde{\mathcal{Z}}_1 \supset \mathcal{Z}_0 = \mathcal{Z}$. To this end, it is only required to prove that $\tilde{\mathcal{Z}}_1 \supseteq \mathcal{Z}$ as $\mathcal{Z}_1 \supset \mathcal{Z}$ holds true because of Lemma 1. The latter statement follows by means of the positive invariance of $\mathcal{Z}$ and $\mathcal{X}$. In fact, for all pairs $(x', g') \in \mathcal{Z}$,

$$\begin{array}{lcll} & x' \in \mathcal{X} & & \\ & \Downarrow & & \\ \bar{x}(k, x', g') & \in & \mathcal{X} \equiv \mathcal{X}_0 & \forall k \in \mathbb{Z}_+ \\ & \Downarrow & & \\ \bar{x}(k, x', g') & \in & \mathcal{X}_0 & \forall k \geq \tau_1 \end{array}$$

Then, $(x', g') \in \mathcal{Z} \Rightarrow (x', g') \in \tilde{\mathcal{Z}}_1$. □

4. Simulations

4.1. Example 1

In this example a system in form of (1) has been considered with matrices

$$\Phi = \begin{bmatrix} 0.3 & 0.8 \\ 0 & 0.5 \end{bmatrix}, G = \begin{bmatrix} 0.718 & 0 \\ 0 & 0.051 \end{bmatrix}, G_d = 0.1 I_2$$

$$H_y = \begin{bmatrix} 0.975 & -1.114 \\ 0 & 9.739 \end{bmatrix}, H_c = \begin{bmatrix} 1.0 & 0.1 \\ 0.1 & 1.0 \end{bmatrix}, L = [L] = \begin{bmatrix} 0 & 0 \\ 0 & 0 \end{bmatrix},$$

A disturbance signal has been taken into account belonging to the following set $\mathcal{D} := \{d \in \mathbb{R} : [1, -1]^T d \leq [5, 5]^T\}$ and satisfying assumption (4) with $\bar{\Delta}_d = 0.1$. Moreover, the variable $c(t)$ is constrained to belong to the set

$$\mathcal{C} := \left\{ c \in \mathbb{R}^2 : \begin{bmatrix} 1 & 0 & -1 & 0 \\ 0 & 1 & 0 & -1 \end{bmatrix}^T c \leq [2, 2, 2, 2]^T \right\}$$

A **RBD-CG** scheme has been designed by means of Algorithm 2 with input $k_0 = 10$ and $\delta = 10^{-5}$. Such an algorithm returned as output the family sets $\mathcal{D}_i := [-0.2(i+1), 0.2(i+1)]$, $i = 1, \dots, 9$, sets $\{\bar{\mathcal{Z}}_i\}_{i=0}^8$ included into $\mathbb{R}^4$ and parameters $\tau_i = 4$, $i = 1, \dots, 9$, $\tau_d^i = 6$, $i = 1, \dots, 9$.

For the sake of clarity, in Fig. 5 we have also reported the constraint sets $\mathcal{W}_\delta^0$, $\mathcal{W}_\delta^8$ and $\mathcal{C}_\delta^0$, $\mathcal{C}_\delta^8$, that have been processed within Algorithm 2.

Moreover, the same figure presents the feasible state sets $\mathcal{X}_i$ defined in (23). From this figures, a first remarkable difference arises between the standard **CG** scheme and the proposed **RBD-CG** one. In fact, since the standard **CG** scheme is conceived only for disturbance worst-case scenarios, it is designed according to the more conservative constraint sets $\mathcal{W}_\delta^0$, $\mathcal{C}_\infty^0$ and $\mathcal{X}_0$. On the contrary the proposed **RBD-CG** adapts its action on the current disturbance magnitude and can operate with less conservative constraint sets. All the computations have been performed on a Apple M1 Macbook Pro through the simulation software Matlab.

Both schemes have been compared by simulations, where the goal was to track the constant reference $r(t) = [3.5, 17.5]^T$ starting from zero initial conditions and under the action of the disturbance signal depicted in Fig. 6. The results are depicted in Figs. 7–8. As expected, both strategies are able to keep the constrained variable in the prescribed range. However, the performance of the **RBD-CG** scheme, quantified by the following instantaneous tracking performance index (the lower, the better)

$$J_{ex1\%}(t) := 100 \times \frac{1}{2}\left(\frac{|r_1(t) - y_1(t)|}{|r_1(t)|} + \frac{|r_2(t) - y_2(t)|}{|r_1(t)|}\right) \tag{44}$$

are better up to the time instant $t = 45$ when, due to the increased magnitude of the disturbance, the switching signal becomes $\sigma(t) = 0$ and both strategies behave in the same way.

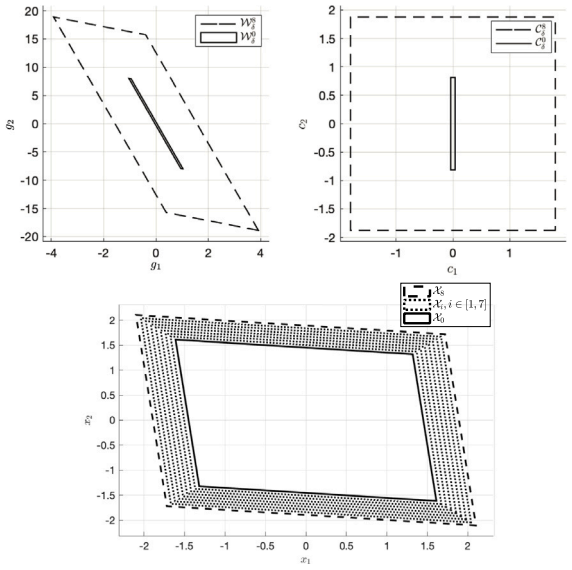


Fig. 5. Example 1: Example 1: (up-left) steady-state admissible reference sets in (21), (up-right) constraints sets (20) after recursions. (bottom) Admissible state sets $\mathcal{X}_i$.

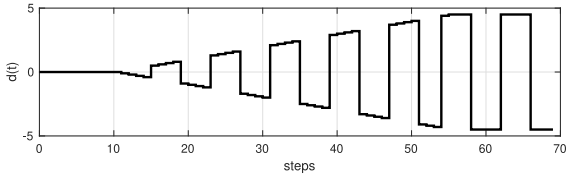


Fig. 6. Example 1: Disturbance in Scenario 1.

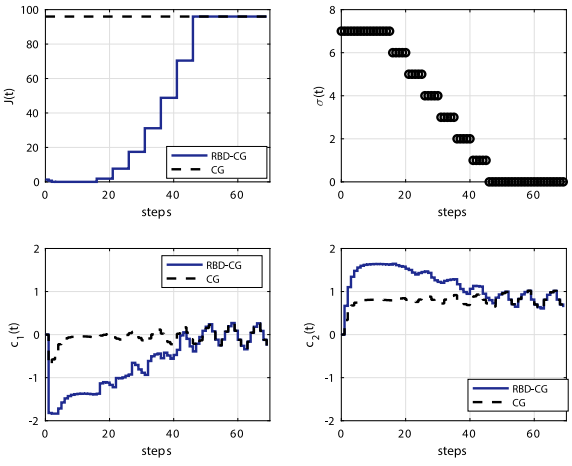


Fig. 7. Example 1: (top left) Optimization cost $J(t)$ related to problems (40)–(41), (top right) switching signal, (bottom) constrained variables.

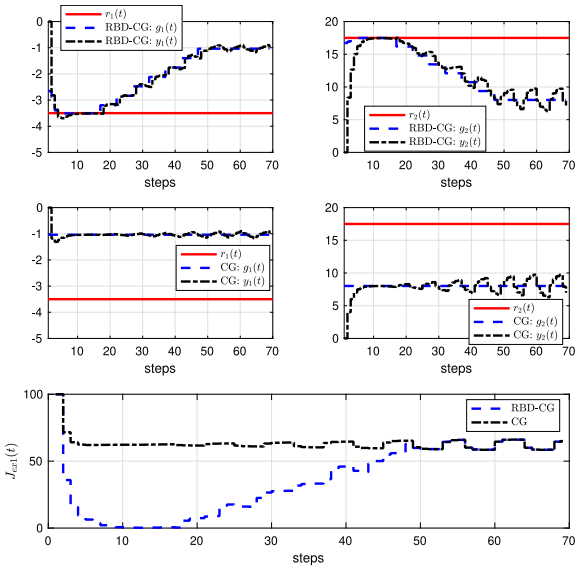


Fig. 8. Example 1: (top) System's output under RBD-CG action, (middle) System's output under CG action, (bottom) Performance index (44).

4.2. Example 2: Position servomechanism

In this second example, the presented strategy has been applied to a servomechanism subject to load disturbance induced by degradation processes. In the context of mass-producing DC motors or similar devices, it is possible to have some level of predictability regarding the disturbance torque signals, including their rate bounds. In fact, in mass production, standardized manufacturing processes are used, which ensures that all motors are produced with the same specifications and materials. This consistency can help to predict the typical performance characteristics, including the behavior of disturbance torque signals. As a result, manufacturers can often determine approximate bounds on the rate of torque disturbances based on statistical data from production batches. Moreover, extensive testing during the production process allows manufacturers to identify common patterns of disturbance and degradation.

For our purposes, consider the position servomechanism schematically described in Fig. 9. It consists of a DC-motor, a gear-box, an elastic shaft and an uncertain load. All system parameters considered in the simulations are reported in Table 1 for completeness. Let θ_M and θ_L denote respectively the motor and the load angles and set

$$x_p = \begin{bmatrix} \theta_L & \dot{\theta}_L & \theta_M & \dot{\theta}_M \end{bmatrix}'$$

Then, the model can be described by the following state-space representation

$$\begin{cases} \dot{x} &= \begin{bmatrix} 0 & 1 & 0 & 0 \\ -\frac{k_\theta}{J_L} & -\frac{\beta_L}{J_L} & \frac{k_\theta}{\rho J_L} & 0 \\ 0 & 0 & 0 & 1 \\ \frac{k_\theta}{\rho J_M} & 0 & -\frac{k_\theta}{\rho^2 J_M} & -\frac{\beta_M + k_T^2/R}{J_M} \end{bmatrix} x + \begin{bmatrix} 0 \\ 0 \\ 0 \\ \frac{k_T}{RJ_M} \end{bmatrix} V + \begin{bmatrix} 0 \\ -1/J_L \\ 0 \\ 0 \end{bmatrix} T_d \\ \theta_L &= \begin{bmatrix} 1 & 0 & 0 & 0 \end{bmatrix} x, \; T = \begin{bmatrix} k_\theta & 0 & -\frac{k_\theta}{\rho} & 0 \end{bmatrix} x \end{cases}$$

The system is recast into a discrete-time model with sampling time $T_s = 0.1s$. A digital controller is then employed having the following transfer function from $e = (r - \theta_L)$ to V

$$G_c(z) = \frac{1000 \cdot \left(9.7929z^3 - 2.1860z^2 - 7.2663z + 2.5556\right)}{10z^4 - 2.7282z^3 - 3.5585z^2 - 1.3029z - 0.0853}$$

The latter is able to reject constant torque disturbance $T_d(t)$ while guaranteeing good tracking performance.

Moreover, such a torque disturbance is assumed to belong to the following set $D := \{d \in \mathbb{R} : [1, -1]^T d \leq [16.5, 16.5]^T\}$ and it assumed to fulfill assumption (4) with $\bar{\Delta}_d = 1.5$.

Starting from this premises, we have designed an **RBD-CG** scheme by means of Algorithm 2 with design parameters $k_0 = 21$ and $\delta = 10^{-5}$. Such an algorithm returned as output the set family $D_i := [-1.5(i+1), 1.5(i+1)]$, $i = 0, \ldots, 10$ and parameters $\tau_i = 9$, $i = 1, \ldots, 10$, $\tau_d^i = 11$, $i = 1, \ldots, 11$. Moreover, generated sets $\{\mathcal{Z}\}_{i=0}^{10}$ are included into $\mathbb{R}^9$ and are computed on the basis of the sets $\mathcal{W}_\delta^i = \mathbb{R}, i = 0, \ldots, 10$ because the resulting matrix $H_c(I_n - \Phi)^{-1}G$ in (6) is $[0, 0]^T$ and sets C_δ^i, $i = 0, \ldots, 10$ are those depicted in Fig. 10.

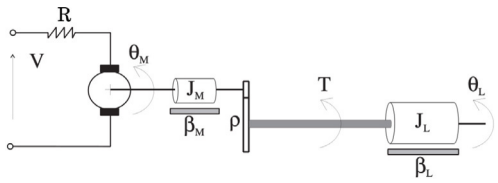


Fig. 9. Servomechanism model.

Table 1
Model parameters.

Symbol	Value (MKS)	Meaning
L_S	1.0	Shaft length
d_S	0.02	Shaft diameter
J_S	Negligible	Shaft inertia
J_M	0.5	Motor inertia
β_M	0.1	Motor viscous friction coefficient
R	20	Resistance of armature
K_T	10	Motor constant
ρ	20	Gear ratio
k_θ	1280.2	Torsional rigidity
J_L	$20J_M$	Load inertia
β_L	25	Load viscous friction coefficient
T_s	0.1	Sampling time

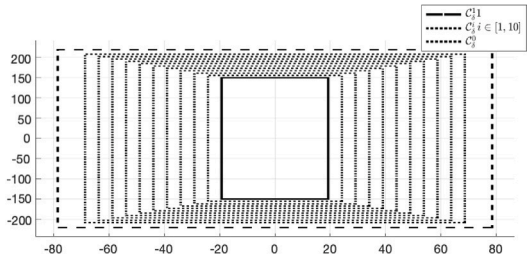


Fig. 10. Example 2: constraints sets (20) after recursions 4.

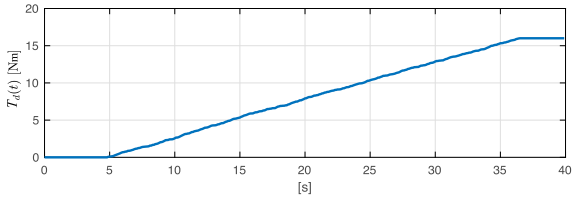


Fig. 11. Example 2: Load disturbance.

The objective of this example is that θ_l tracks a desired square wave signal $r(t)$ with amplitude $\pi/2$ and period 20[s] (please refer to Fig. 12 red solid lines), ensuring that the torque and input voltage constraints are fulfilled for all time instant under the action of the CG scheme. Furthermore, during the simulations, it is assumed that the disturbance torque increases, as illustrated in Fig. 11.

The proposed RBD-CG has been compared with the traditional CG scheme implemented, as usual, by assuming a worst-case scenario on the disturbance, i.e. $T_d(t) \in \mathcal{D}_0$. This scheme is here referred to as **CG(worst)**. A further CG scheme, considered as a counterpart, is designed in the best-case scenario, that is $T_d(t) \in \mathcal{D}_{10}$, and is here referred as **CG(best)**.

The results are shown in Figs. 12–13. As in the previous example, **RBD-CG** consistently outperforms **CG(worst)** that exhibits reduced performance even in the best-case scenario. However, the ability of the proposed approach to reduce conservativeness leads to the use of more active control adjustments based on the estimated disturbance (see Fig. 13).

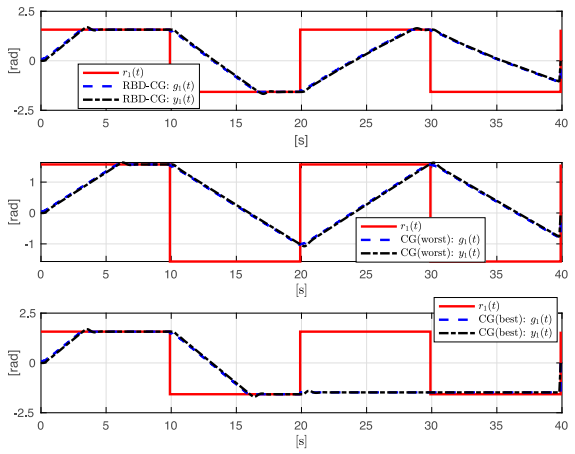


Fig. 12. Example 2: (top) Output performance of RBD-CG, (middle) Output performance of CG(worst), (bottom) Output performance of CG(best).

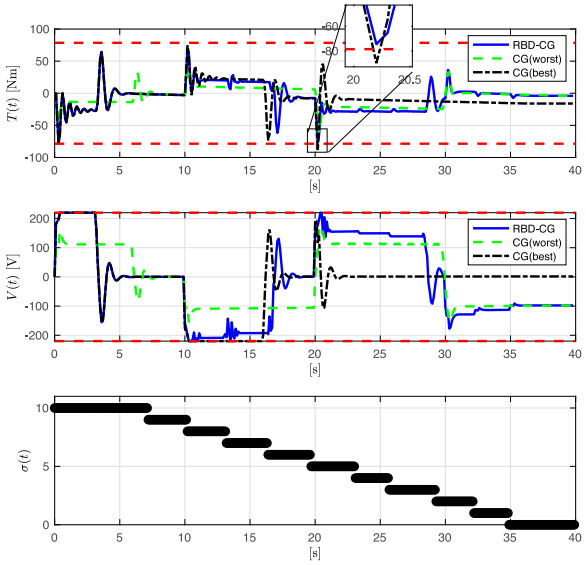


Fig. 13. Example 2: (top left) Optimization cost $J(t)$ related to problems (40)–(41), (top right) switching signal, (bottom) constrained variables.

On the other hand, as expected, **CG(best)** demonstrates excellent performance, maintaining robustness up to time instant $t = 20.2$ [s]. At this point, a constraint violation on the torque occurs, preventing the scheme from finding a feasible solution for $g(t)$. Consequently, to avoid potential damage, the last computed solution is applied from that moment onward, and the system is no longer able to track the angle reference $r(t)$.

Furthermore, the comparison analysis was extended to the computational aspects, with the results reported in Table 2 that highlights the key aspects of this comparison in the scenario presented above. It is interesting to observe that, while **RBD-CG** relies on a higher off-line CPU time, this extra computational burden is not a significant design concern, as off-line computations are typically performed during the design phase and do not impact real-time performance. The complexity added by handling rate-bounded disturbances is justified by the improvement of the overall tracking performance of the system. In fact, the **RBD-CG** scheme significantly outperforms the traditional **CG** one in terms of tracking accuracy as testified by the value of the average index $J_{ex1}(t)$ in (44). This substantial improvement is obtained at the price of a very slight increase in the average online computational time for **RBD-CG**. In fact, the latter quantity remains comparable to that of

Table 2
Example 2: A complete quantitative comparison between CG and RBD-CG.

	RBD-CG	CG (worst)	CG (best)
Off-line CPU time [s]	187.21	19.57	19.35
Avg. On-line CPU time [s/step]	0.24	0.22	0.23

CG. This shows that the real-time implementation of **RBD-CG** is highly efficient, despite the added complexity of dealing dynamically with disturbances. The slight increase in on-line computation is negligible in practical applications, ensuring that the system can operate smoothly in real-time.

5. Conclusions

In this paper, a novel CG scheme has been introduced for solving the reference management problem in linear systems subject input/state constraints. In particular, the traditional CG scheme of [2] has been here equipped with the capability of dealing with rate-bounded disturbances acting as non-manipulable inputs on the plant. As one of its main merits, the proposed scheme is capable to take care of non-manipulable inputs affecting the plant by on-line exploiting the Command Governor viability properties and transition dwell-time concepts. The applicability and effectiveness of the proposed control scheme have been assessed through simulations that have put in evidence that the RBD-CG presents an enlarged set of admissible states with respect to traditional CG.

CRediT authorship contribution statement

Francesco Tedesco: Writing – review & editing, Writing – original draft, Supervision, Methodology, Investigation, Formal analysis, Conceptualization. **Gianfranco Gagliardi:** Writing – review & editing, Writing – original draft, Visualization, Validation, Software, Project administration, Data curation. **Alessandro Casavola:** Writing – review & editing, Writing – original draft, Project administration, Methodology, Funding acquisition.

Declaration of competing interest

The authors declare that they have no known competing financial interests or personal relationships that could have appeared to influence the work reported in this paper.

Acknowledgments

This work has been partially supported by the research project - ID:20225MESZB "Resilient Optimization in Distributed Cyber-Physical Control Problems subject to Adversarial Behaviour" granted by the Italian Ministry of University and Research (MUR), within the PRIN 2022 program, and European Union - Next Generation EU.

Data availability

Data will be made available on request.

References

[1] J.B. Rawlings, D.Q. Mayne, M. Diehl, Model Predictive Control: Theory, Computation, and Design, Nob Hill Publishing Madison, 2017, p. 2.
[2] A. Casavola, E. Mosca, D. Angeli, Robust command governors for constrained linear systems., IEEE Trans. Autom. Control 45 (2000) 2071–2077.
[3] E.G. Gilbert, I. Kolmanovsky, K. Tin Tan, Discrete-time reference governors and the nonlinear control of systems with state and control constraint, International Journal on Robust and Nonlinear Control 5 (1995) 487–504.
[4] E. Garone, S. Di Cairano, I. Kolmanovsky, Reference and command governors for systems with constraints: A survey on theory and applications, Automatica 75 (2017) 306–328.
[5] I. Kolmanovsky, U. Kalabic, E. Gilbert, Developments in constrained control using reference governors, IFAC Proc. Vol. 45 (17) (2012) 282–290.
[6] A.B. Açikmeşe, M. Corless, M, Robust tracking and disturbance rejection of bounded rate signals for uncertain/non-linear systems, Internat. J. Control 76 (11) (2003) 1129–1141.
[7] I. Kolmanovsky, E.G. Gilbert, N.H. McClamroch, T.L. Maizenberg, Toward less conservative designs of multimode controllers for systems with state and control constraints, in: Proceedings of the 37th IEEE Conference on Decision and Control 1998, Tampa, FL, 1998.
[8] M. Huang, H. Nakada, K. Butts, I. Kolmanovsky, Robust rate-based model predictive control of diesel engine air path, in: American Control Conference 2014, Portland, OR, 2014.
[9] D. Liberzon, J.P. Hespanha, A.S. Morse, Stability of switched linear systems: A Lie-algebraic condition, Syst. Control Lett. 37 (3) (1999) 117–122.
[10] I. Kolmanovsky, J. Sun, J, A multi-mode switching-based command tracking in network controlled systems with pointwise-in-time constraints and disturbance inputs, in: IEEE. 6th World Congress on Intelligent Control and Automation, vol. 1, 2006, pp. 199–204.
[11] M. Hosseinzadeh, I. Kolmanovsky, S. Baruah, B. Sinopoli, Reference governor-based fault-tolerant constrained control, Automatica 136 (2022) 110089.
[12] D. Famularo, G. Franzè, A. Furfaro, M. Mattei, A hybrid real-time command governor supervisory scheme for constrained control systems, IEEE Trans. Control Syst. Technol. 23 (3) (2015) 924–936.
[13] F. Tedesco, A. Casavola, Load/frequency control in the presence of renewable energy systems: A reference-offset governor approach, in: 21st IFAC World Congress, Berlin, Germany, 2020.
[14] J.P. Aubin, Viability Theory, Birkhauser, Basel, 1991.
[15] E.G. Gilbert, I. Kolmanovsky, Maximal output admissible sets for discrete-time systems with disturbance inputs, in: Proc. of the American Contr. Conf., 1995.
[16] E.G. Gilbert, I. Kolmanovsky, Fast reference governors for systems with state and control constraint and disturbance inputs, Int. J. Robust Nonlinear Control 9 (1999) 1117–1141.
[17] E.G. Gilbert, K. Tin Tan, Linear systems with state and control constraints: The theory and applications of maximal output admissible sets, IEEE Trans. Automat. Control 36 (1991) 1008–1020.